The Journal of Experimental Medicine

The Innate Mononuclear Phagocyte Network Depletes B Lymphocytes through Fc Receptor–dependent Mechanisms during Anti-CD20 Antibody Immunotherapy

Junji Uchida,[1] Yasuhito Hamaguchi,[1] Julie A. Oliver,[1] Jeffrey V. Ravetch,[2] Jonathan C. Poe,[1] Karen M. Haas,[1] and Thomas F. Tedder[1]

[1]*Department of Immunology, Duke University Medical Center, Durham, NC 27710*
[2]*Laboratory of Molecular Genetics and Immunology, The Rockefeller University, New York, NY 10021*

Abstract

Anti-CD20 antibody immunotherapy effectively treats non-Hodgkin's lymphoma and autoimmune disease. However, the cellular and molecular pathways for B cell depletion remain undefined because human mechanistic studies are limited. Proposed mechanisms include antibody-, effector cell–, and complement-dependent cytotoxicity, the disruption of CD20 signaling pathways, and the induction of apoptosis. To identify the mechanisms for B cell depletion in vivo, a new mouse model for anti-CD20 immunotherapy was developed using a panel of twelve mouse anti–mouse CD20 monoclonal antibodies representing all four immunoglobulin G isotypes. Anti-CD20 antibodies rapidly depleted the vast majority of circulating and tissue B cells in an isotype-restricted manner that was completely dependent on effector cell Fc receptor expression. B cell depletion used both FcγRI- and FcγRIII-dependent pathways, whereas B cells were not eliminated in FcR common γ chain–deficient mice. Monocytes were the dominant effector cells for B cell depletion, with no demonstrable role for T or natural killer cells. Although most anti-CD20 antibodies activated complement in vitro, B cell depletion was completely effective in mice with genetic deficiencies in C3, C4, or C1q complement components. That the innate monocyte network depletes B cells through FcγR-dependent pathways during anti-CD20 immunotherapy has important clinical implications for anti-CD20 and other antibody-based therapies.

Key words: lymphoma • therapy • autoimmune diseases • mouse model • Rituximab

Introduction

B lymphocytes are the origin of humoral immunity, represent a substantial portion of hematopoietic malignancies, and contribute to autoimmunity. Consequently, cell surface molecules expressed by B cells and their malignant counterparts are important targets for immunotherapy. CD20, a B cell–specific member of the MS4A gene family with four membrane-spanning domains, is expressed on the surface of immature and mature B cells and their malignant counterparts (1). Chimeric or radiolabeled mAb-based therapies directed against CD20 represent an effective treatment for non-Hodgkin's lymphoma (2–6). Clinical studies indicate that anti-CD20 mAb therapy also ameliorates the manifestations of rheumatoid arthritis, idiopathic thrombocytopenic purpura, and hemolytic anemia, as well as other immune-mediated diseases (7, 8). Despite the effectiveness of this therapy, relatively little is known about why CD20 is such a potent target molecule for therapy. Moreover, the precise molecular and cellular mechanisms for B cell depletion and tumor regression after anti-CD20 mAb treatment and the development of resistance to anti-CD20 immunotherapy remain uncertain (9).

Competing hypotheses are used to explain the therapeutic efficacy of anti-CD20 mAbs in vivo. In one model, CD20 serves as a membrane-embedded target for mAb-mediated depletion of B cells through activation of the innate immune system or the initiation of effector mechanisms (10–12). Thus far, major effector mechanisms include C- and Ab-dependent cytotoxicity (10, 13). Rituximab, a chimeric human IgG1 anti–human CD20 mAb is highly effective in inducing classical pathway C activation and C-dependent cytotoxicity of freshly isolated lymphoma cells and B cell

J. Uchida and Y. Hamaguchi contributed equally to this work.

Address correspondence to Thomas F. Tedder, Department of Immunology, Box 3010, Room 353 Jones Building, Research Drive, Duke University Medical Center, Durham, NC 27710. Phone: (919) 684-3578; Fax: (919) 684-8982; email: thomas.tedder@duke.edu

Abbreviation used in this paper: PI, propidium iodide.

 J. Exp. Med. © The Rockefeller University Press • 0022-1007/2004/06/1659/11 $8.00
Volume 199, Number 12, June 21, 2004 1659–1669
http://www.jem.org/cgi/doi/10.1084/jem.20040119

lines (10, 14–17). Rituximab also activates C in vivo in both patients (18) and primates (19). Furthermore, tumor cell expression of C regulatory proteins, including CD59, is associated with resistance to anti-CD20 therapy (14, 20). Although many consider C-dependent cytotoxicity to be the major pathway used by Rituximab to deplete human lymphoma cells in vitro and in vivo (14–16, 21–23), others have found that the susceptibility of tumor cells to C-mediated lysis and expression of C inhibitors CD46, CD55, and CD59 on tumor cells does not predict the outcome of Rituximab therapy (24). Other Ab-dependent effects also appear important because a chimeric anti-CD20 mAb of an isotype different than that used clinically does not deplete normal B cells in nonhuman primates (25) and the antitumor effect of anti-CD20 mAb depends in part on immune activation through Fc receptors (FcγR) for IgG (26). Alternatively, anti-CD20 mAb treatment alters transmembrane Ca^{2+} transport and B cell function, which disrupts progression through cell cycle (1) and can induce B cell apoptosis (13, 27). It is difficult to differentiate between these hypotheses in vivo due to the complexities of carrying out mechanistic studies in humans undergoing immunotherapy (9). Moreover, human studies primarily focus on changes in blood, which contains <2% of the B cells outside of the BM. Thus, it is difficult to accurately ascertain the effects of anti-CD20 therapies on the majority of B cells, which are found in peripheral lymphoid tissues. As with human CD20, mouse CD20 is also B cell specific, being first expressed during the pre–B to immature B cell transition, with continued expressed during maturation until plasma cell differentiation (28). Therefore, to examine how mAb binding to CD20 initiates effector systems that lead to B cell depletion, we developed a unique panel of mouse anti–mouse CD20 mAbs (28). We have used these mAbs to establish a preclinical mouse model of anti-CD20 mAb immunotherapy amenable to mechanistic studies and genetic manipulation. This model has allowed a comparison between the existing in vitro and in vivo data that shape current models of how anti-CD20 therapies work, and has resulted in mechanism-based predictions of the biological outcome of mAb therapy in vivo.

Materials and Methods

Abs and Immunofluorescence Analysis. Mouse CD20–specific mouse mAbs were as described previously (28). Other mAbs included the following: CD19 mAb MB19-1 (29), B220 mAb RA3-6B2 (provided by R. Coffman, DNAX Corp., Palo Alto, CA), and Thy1.2 mAb (Caltag Laboratories). Isotype-specific and anti–mouse Ig or IgM Abs were from Southern Biotechnology Associates, Inc. Single cell leukocyte suspensions were stained on ice using predetermined optimal concentrations of each Ab for 20–60 min as described previously (30). Cells with the forward and side light scatter properties of lymphocytes were analyzed on FACScan™ or FACSCalibur™ flow cytometers (Becton Dickinson). Background staining was determined using unreactive control mAbs (Caltag Laboratories) with gates positioned to exclude ≥98% of the cells.

Mice. $CD20^{-/-}$ and WT littermates were as described previously (28). $Fc\gamma RI^{-/-}$ and $Fc\gamma RIII^{-/-}$ mice were as described previously (31). C57BL/6, $Fc\gamma RII^{-/-}$ (B6,129S-Fcgr2tm1Rav), $Fc\gamma RIII^{-/-}$ (C57BL/6-Fcgr3tm1Sjv), Beige (C57BL/6-*Lyst*$^{bg/bg}$), $Perforin^{-/-}$ (C57BL/6-Pfptm1Sdz), CSF1^{op} (*Csf1*^{op}), and nude (C57BL/6-*Hfh11*^{nu}) mice were from The Jackson Laboratory. FcR common γ chain (FcRγ)-deficient mice ($FcR\gamma^{-/-}$, B6.129P2-*Fcerg1*^{tm1}) were from Taconic Farms. $C1q^{-/-}$ mice as described previously (32) were provided by G. Kelsoe (Duke University, Durham, NC) with the permission of M. Walport (Imperial College, London, UK). $LAT^{-/-}$ mice were from W. Zhang (Duke University, Durham, NC; reference 33). $C3^{-/-}$ and $C4^{-/-}$ mice were from M. Carroll (Center for Blood Research, Boston, MA; reference 34). Macrophage-deficient mice were generated by tail vein injections of clodronate-encapsulated liposomes (0.1 ml/10 g body weight; Sigma-Aldrich) on days −2, 1, and 4 as described previously (35). All mice were housed in a specific pathogen-free barrier facility and first used at 2–3 mo of age. These studies were approved by the Animal Care and Use Committee of Duke University.

Immunotherapy. Sterile anti–mouse CD20 and isotype control mAbs (0.5–250 μg) in 200 μl PBS were injected through lateral tail veins. All experiments used 250 μg mAb unless indicated otherwise. Blood and spleens were collected at 1 h and 2, 4, 7, 28, 48, 50, 52, 54, 56, or 58 d after treatment. Blood leukocyte numbers were quantified by hemocytometer after red cell lysis, with $B220^+$ B cell frequencies determined by immunofluorescence staining with flow cytometry analysis. Ab doses in humans and mice were compared using the Oncology Tool Dose Calculator (www.fda.gov/cder/cancer/animalframe.htm).

C Assays. WT mouse spleen B cells were purified (>93% $B220^+$) by T cell removal using Thy1.2 mAb-coated magnetic beads (Dynal). Quantification of C-mediated B cell killing in vitro was as described previously (36). Spleen B cells were incubated with each anti-CD20 mAb (0.5 μg/ml) and baby rabbit C (diluted 50-fold; GIBCO BRL) for 2 h at 37°C. PBS was added to each tube with incubation for 4 h at 37°C before the cells were washed and stained with propidium iodide (PI) and anti-B220 mAb. PI exclusion was determined by flow cytometry analysis.

Statistical Analysis. All data are shown as means ± SEM. The Student's *t* test was used to determine the significance of differences between population means.

Results

Anti-CD20 mAb Depletion of B Cells In Vivo. 12 mouse anti–mouse CD20 mAbs, with representatives of each IgG isotype, were assessed for their ability to bind B cells and deplete them in vivo. Each mAb reacted uniformly with $CD19^+$ primary B cells in vitro with characteristic mean fluorescence intensities that were independent of mAb isotype (Fig. 1 A; not depicted). When mAb reactivity with primary B cells was assessed over a range of mAb concentrations, most mAbs reached saturating levels of staining when used at concentrations between 1–10 μg/ml (Fig. 1 B; not depicted). On average, 50% maximal log mAb staining was achieved at mAb concentrations of ∼0.5 μg/ml (Fig. 1 B, arrows). When all mAbs were used at 0.5 μg/ml, each mAb reacted uniformly with $CD19^+$ primary B cells with characteristic low to high mean fluorescence intensities (Fig. 1 C and Table I). Similar results were obtained using a mouse

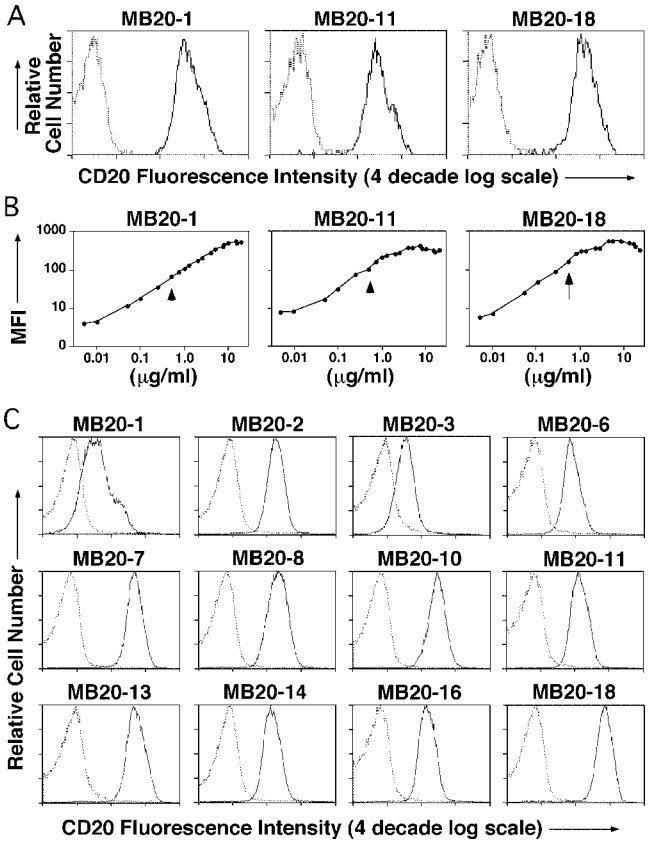

Figure 1. Reactivity of anti-CD20 mAbs with spleen B cells. (A) Fluorescence intensity of $CD19^+$ cells stained with representative anti-CD20 (solid lines) or isotype-matched control (dashed line) mAbs (10 μg/ml). (B) Mean fluorescence intensity (MFI) of anti-CD20 mAb staining over a range of mAb concentrations. Arrows indicate mean intensities of mAb staining when used at 0.5 μg/ml. (C) Fluorescence intensity of $CD19^+$ cells stained with anti-CD20 (solid lines) or isotype-matched control (dashed line) mAbs (0.5 μg/ml). In all cases, mAb staining was visualized using PE-conjugated isotype-specific secondary Abs with flow cytometry analysis. Results represent those obtained in three or more experiments.

CD20 cDNA-transfected pre–B cell line with anti–mouse Ig secondary antibody (unpublished data). Based on this analysis, the MB20-1 mAb represented mAbs with the lowest relative affinity/avidity, whereas the MB20-18 mAb reacted strongly with B cells and stained B cells at the highest levels of all 12 anti-CD20 mAbs (Table I). Thus, each mAb reacted specificity with B cells and displayed reasonable binding characteristics as assessed by flow cytometry.

Each anti–mouse CD20 mAb was given to mice at 250 μg/mouse, a single dose ~10-fold lower than the 375 mg/m^2 dose primarily given four times for anti-CD20 therapy in humans (2–6). Under these conditions, multiple mAbs had potent and long-lasting effects on peripheral B cell numbers, whereas other mAbs had heterogeneous in vivo effects (Fig. 2). The effectiveness of mAb-induced B cell depletion from the circulation by day 2 and spleen by day 7 correlated closely with mAb isotype (Table I and Fig. 2, A and B), with IgG2a > IgG1 > IgG2b > IgG3. MB20-11 and other IgG2a mAbs (MB20-6 and MB20-16) depleted >95% of blood B cells and ~93% of splenic B cells. The few remaining peripheral B cells primarily represented phenotypically immature cells emerging from the BM (unpublished data). The MB20-11 mAb depleted significant numbers of circulating B cells when given as a single dose as low as 0.5 μg/mouse, whereas significant depletion of spleen B cells by day 7 required a fivefold higher mAb dose of 2.5 μg/mouse (Fig. 2 C). Equally striking was the finding that a single injection of MB20-11 mAb depleted circulating B cells within 1 h of mAb treatment, with a durable effect for ~57 d before B cells began to repopulate the circulation and spleen (Fig. 2 D). By contrast, none of the mAbs had significant effects when given to $CD20^{-/-}$ mice and isotype-control mAbs given under identical conditions did not affect B cell numbers (Fig. 2; not depicted). Likewise, circulating and tissue $Thy1.2^+$ T cell numbers were unchanged in anti-CD20 mAb-treated mice (Fig. 2 A; unpublished data), consistent with B cell–restricted CD20 expression (28).

Table I. *Mouse Anti–Mouse CD20 mAbs*

Isotype	Ab	B cell reactivity[a]	Percent in vivo depletion[b]	
			Blood	Spleen
IgG1	MB20-1	69	95 ± 3	93 ± 3
	MB20-2	209	88 ± 1	67 ± 8
	MB20-14	166	94 ± 4	77 ± 8
IgG2a	MB20-6	96	99 ± 1	93 ± 5
	MB20-11	158	98 ± 1	92 ± 2
	MB20-16	170	99 ± 1	95 ± 0
IgG2b	MB20-7	525	82 ± 9	36 ± 36
	MB20-8	240	94 ± 1	3 ± 18
	MB20-10	317	91 ± 1	3 ± 9
	MB20-18	729	96 ± 1	74 ± 3
IgG3	MB20-3	47	1 ± 1	1 ± 3
	MB20-13	603	18 ± 1	3 ± 1

[a]Values represent the mean linear fluorescence intensity for immunofluorescence staining of spleen $CD19^+$ B cells with 0.5 μg/ml of each MB20 mAb (see Fig. 1 C). Splenocyte staining was visualized using isotype-specific secondary Abs. Control staining was ≤6 in all cases.
[b]Values (± SEM) indicate the percent of $B220^+$ B cells depleted from blood or spleen 7 d after mAb treatment ($n \geq 3$) compared with isotype-matched control mAbs.

Role for FcγR in B Cell Depletion. The role of the innate immune system in B cell depletion by anti-CD20 mAb treatment was assessed using FcγR-deficient mice (37). Mouse effector cells express three different FcγR classes for IgG: the high affinity FcγRI (CD64), and the low affinity FcγRII (CD32) and FcγRIII (CD16) molecules (38). FcγRI and FcγRIII are hetero-oligomeric complexes in which the respective ligand-binding α chains associate with a common γ chain (FcRγ). FcRγ chain expression is required for FcγR assembly and for FcγR triggering of effector functions, including phagocytosis by macrophages and cytotoxicity by NK cells (37). High af-

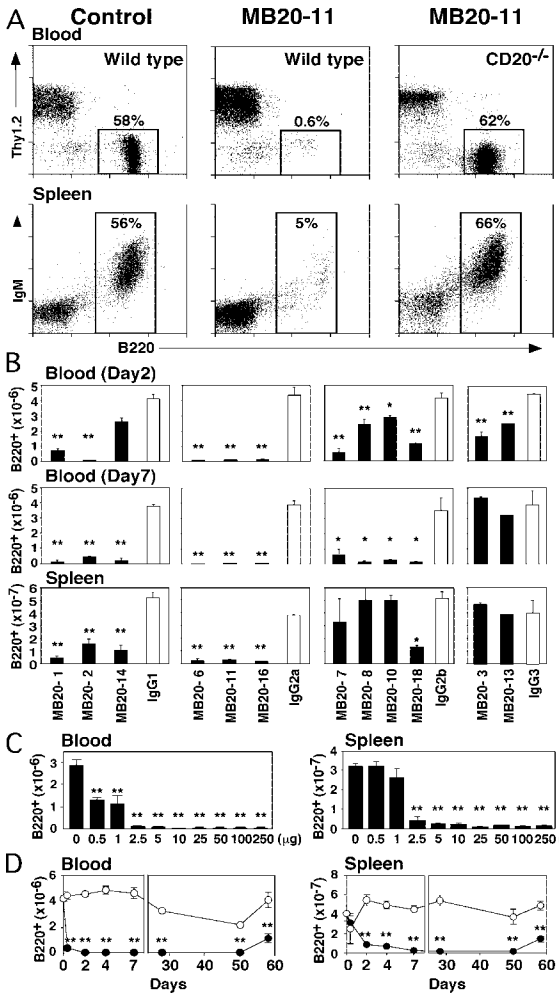

Figure 2. B cell depletion in vivo. (A) Representative B cell depletion from blood (day 2) and spleen (day 7) after MB20-11 or isotype-matched control mAb treatment of WT or $CD20^{-/-}$ mice as determined by immunofluorescent staining with flow cytometry analysis. Numbers indicate the percentage of gated $B220^+$ B cells. (B) Total numbers (± SEM) of blood (days 2 or 7, per ml) and spleen (day 7) B cells after treatment of two or more WT littermates with MB20 or isotype control mAbs. Significant differences between mean results for MB20 or isotype control mAb–treated mice are indicated. *, $P < 0.05$; **, $P < 0.01$. (C) Blood and spleen B cell numbers (± SEM) in WT littermates 7 d after treatment with MB20-11 mAb at different doses (two or more mice per data point). Significant differences between untreated (0) and mAb-treated mice are indicated. **, $P < 0.01$. (D) Blood and spleen B cell numbers (± SEM) in WT mice after MB20-11 (●) or isotype control (○) mAb treatment on day 0 (five or more mice per group). The value shown after time 0 represents data obtained at 1 h.

finity FcγRI preferentially binds monomeric IgG2a > IgG2b > IgG3/IgG1, whereas the two low affinity receptors bind polymeric IgGs of different isotypes (39). FcγRIII binds IgG2a > IgG1 > IgG2b >> IgG3 (39).

In contrast to almost complete B cell depletion in WT mice (Fig. 2), MB20-11 mAb treatment reduced circulating B cell numbers by only 20–35% in $FcR\gamma^{-/-}$ mice over 4 d (Fig. 3 A), with no effect from days 7 to 18 (unpublished data). Moreover, MB20-11 mAb treatment actually increased spleen B cell numbers in $FcR\gamma^{-/-}$ mice compared with control mAb–treated littermates (Fig. 3, B and C), predominantly due to increased numbers of immature B cells (unpublished data). An isotype-matched control mAb had no significant effect in $FcR\gamma^{-/-}$ mice. In $Fc\gamma RI^{-/-}$ mice, the MB20-11 mAb induced an initial decrease in B cell numbers at 1 h, but incomplete depletion of circulating B cells on day 2. MB20-11 mAb treatment only partially depleted B cells in $Fc\gamma RI^{-/-}$ mice with 21% of spleen B cells persisting at day 7 compared with control mAb–treated littermates. By contrast, the MB20-11 mAb depleted circulating and tissue B cells by ≥95% in WT, $Fc\gamma RII^{-/-}$, and $Fc\gamma RIII^{-/-}$ mice by day 7. Identical results were obtained using two independent $Fc\gamma RIII^{-/-}$ mouse (31, 40) lines (unpublished data). B cell depletion by the IgG1 MB20-1 and IgG2b MB20-18 mAbs was similarly affected by FcRγ chain deficiency. Circulating B cells were not significantly reduced by MB20-1 mAb treatment of $FcR\gamma^{-/-}$ mice, whereas circulating B cells were depleted in WT mice (Fig. 3 D). Likewise, spleen B cells were not significantly reduced by MB20-1 mAb treatment of $FcR\gamma^{-/-}$ mice, whereas spleen B cell numbers were reduced by 93% in WT mice. Circulating B cells were significantly reduced by MB20-18 mAb treatment of $FcR\gamma^{-/-}$ mice, but not to the same extent as occurred in WT mice (Fig. 3 E). However, spleen B cells were not significantly reduced by MB20-18 mAb treatment of $FcR\gamma^{-/-}$ mice, whereas spleen B cell numbers were reduced by 74% in WT mice. Thus, anti-CD20 mAb therapy primarily depleted B cells through pathways that require FcRγ chain expression.

C Does Not Facilitate B Cell Depletion. Because C activation is considered a major mechanism for B cell depletion during anti-CD20 mAb therapy, the role of C in B cell depletion by anti-CD20 mAb treatment was assessed using C-deficient (34) and C1q-deficient (32) mice. The C-activating ability of each anti-CD20 mAb was first assessed in vitro. In the presence of C, most of the anti-CD20 mAbs induced significant B cell lysis as indicated by PI uptake relative to isotype-matched control mAbs, although cytotoxic capability varied between Abs (Fig. 4 A). Without C, none of the anti-CD20 mAbs induced B cell PI uptake or apoptosis during these in vitro assays (unpublished data). The MB20-18 mAb initiated the most potent C-dependent lysis of B cells, although the MB20-11 mAb was also effective in inducing significant C-mediated B cell lysis in vitro. However, the ability of each mAb to induce C-dependent B cell killing in vitro did not correlate with the ability of each mAb to deplete B cells in vivo (Fig. 2 B). Moreover, the MB20-11 mAb effectively cleared all blood and >90% of spleen B cells in $C3^{-/-}$ and $C4^{-/-}$ mice (Fig. 4 B). This observation was not mAb isotype specific because the MB20-1 and MB20-18 mAbs effectively depleted blood and spleen B cells to similar extents in both $C3^{-/-}$ and WT mice (Fig. 4, C and D). Thus, anti-CD20 mAb therapy primarily depletes B cells through FcγR-dependent and C3-, C4-, and C1q-independent mechanisms.

Monocytes Mediate B Cell Depletion In Vivo. Because the depleting ability of anti-CD20 mAb treatment correlated di-

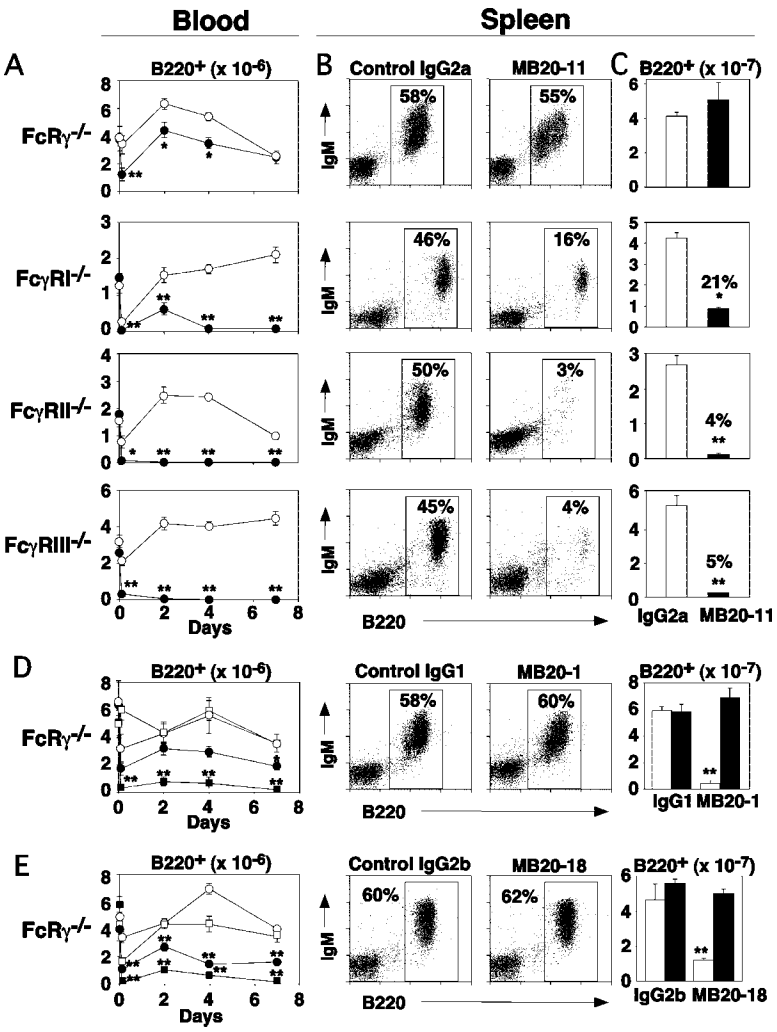

Figure 3. B cell depletion is FcγR dependent. (A) Blood B cell depletion after MB20-11 (●) or isotype control (○) mAb treatment of FcRγ$^{-/-}$, FcγRI$^{-/-}$, FcγRII$^{-/-}$, and FcγRIII$^{-/-}$ mice on day 0. Values indicate mean circulating B cell numbers (± SEM, per ml) before (time 0) and 1 h or 2, 4, or 7 d after mAb treatment (five or more mice per time point). (B) Representative spleen B cell depletion 7 d after mAb treatment. Numbers indicate the percentage of B220$^+$ lymphocytes within the indicated gates. (C) Mean spleen B cell numbers (± SEM) 7 d after MB20-11 (solid bars) or isotype control (open bars) mAb treatment (five or more mice per group). Numbers indicate the mean relative percentage of B220$^+$ lymphocytes in anti-CD20 mAb–treated mice compared with control mAb–treated littermates. (D) B cell depletion after MB20-1 (●) or isotype control (○) mAb treatment of FcRγ$^{-/-}$ littermates on day 0 compared with MB20-1 (■) or isotype control (□) mAb treatment of WT littermates on day 0. Representative spleen B cell depletion 7 d after MB20-1 or control mAb treatment of FcRγ$^{-/-}$ littermates. Numbers indicate the percentage of B220$^+$ lymphocytes. Bar graphs represent mean spleen B cell numbers (± SEM) 7 d after MB20-1 or isotype control mAb treatment of FcRγ$^{-/-}$ (solid bars) or WT (open bars) mice (five or more mice per group). (E) Blood and spleen (day 7) B cell depletion after MB20-18 (●) or isotype control (○) mAb treatment of FcRγ$^{-/-}$ littermates on day 0 compared with MB20-18 (■) or isotype control (□) mAb treatment of WT littermates on day 0. Histograms represent mean spleen B cell numbers (± SEM) 7 d after MB20-18 or isotype control mAb treatment of FcRγ$^{-/-}$ (solid bars) or WT (open bars) mice (five or more mice per group). (A–E) Significant differences between mean results for MB20 or isotype control mAb–treated mice are indicated. *, $P < 0.05$; **, $P < 0.01$.

rectly with mAb isotype and FcγR expression, the contributions of NK cells, T cells, and macrophages to FcγR-mediated B cell depletion was determined. Mice rendered macrophage deficient by treatment with liposome-encapsulated clodronate did not significantly deplete circulating B cells by 1 h after MB20-11 mAb treatment, and had normal numbers of circulating B cells for up to 7 d (Fig. 5 A). Similarly, spleen B cell numbers in clodronate-treated mice were only decreased by 39% on day 7 relative to control mAb–treated littermates (Fig. 5 B). Mice with tissue-specific losses in macrophage subpopulations (41) due to CSF-1 deficiency (CSF-1^{op}) were also slow to clear circulating B cells after MB20-11 mAb treatment, and only depleted 84% of phenotypically mature spleen B cells by day 7 (Fig. 5). By contrast, athymic nude and LAT$^{-/-}$ mice that lack functional T cells (33) depleted >96% of blood and spleen B cells. Likewise, anti-CD20 mAb treatment removed ~95% of circulating and spleen B cells in beige and perforin$^{-/-}$ mice (Fig. 5) with defective NK cell function (42). These findings implicate both CSF-1–dependent and –independent macrophage subsets as the major effector cells for depletion of CD20$^+$ B cells in vivo, and essentially exclude T cell–, NK cell–, and perforin-dependent mechanisms.

Discussion

These studies reveal that the phagocytic network of the innate immune system is primarily responsible for eliminating circulating and tissue B cells after anti-CD20 mAb therapy in mice (Figs. 3 and 5). Likely mechanisms for B cell depletion include FcγR-mediated phagocytosis of mAb-coated B cells or the secretion of cytolytic or unknown cytotoxic factors by activated macrophages. Macrophages activated by FcγR-dependent pathways may also release inflammatory cytokines and recruit cytotoxic T lymphocytes, NK cells, and neutrophils that contribute to B cell depletion and amplify local inflammatory responses. A role for FcγRI/III$^+$ CD11b$^+$ (phagocytic) cells has been demonstrated for mAb-induced solid tumor regression, with the conclusion that activated macrophages induce the expansion of tumor-eliminating cytotoxic T cells (43). However, T cells and NK cells did not play a measurable role in B cell depletion after anti-CD20 mAb treatment (Fig. 5). CD20-directed therapy is largely thought to also involve C activation (16), and the anti-CD20 mAbs used in this study activate C in vitro (Fig. 4 A). However, there was no evidence that classical or alternative pathway C ac-

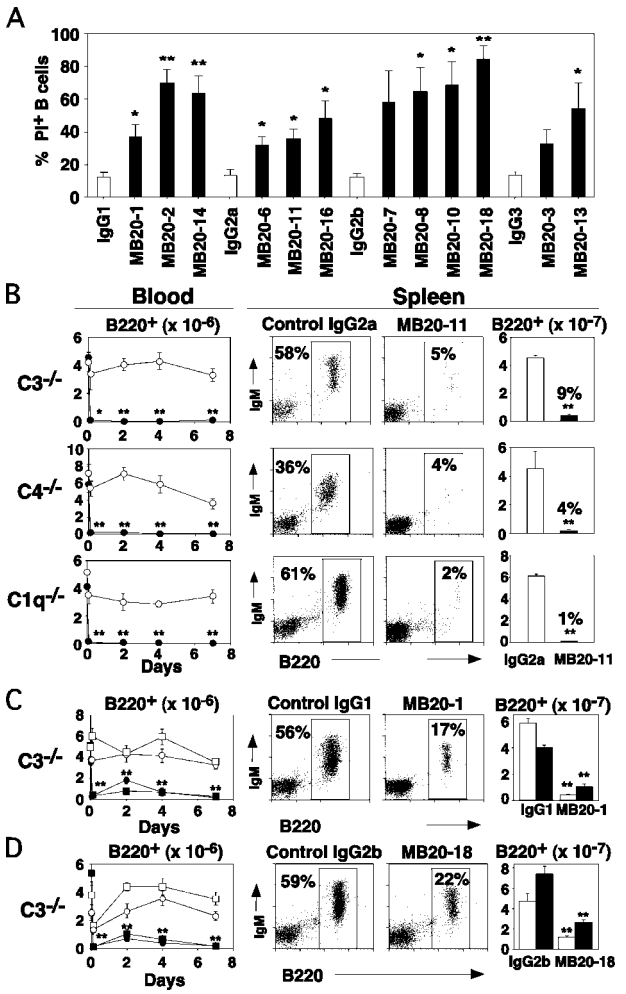

Figure 4. B cell depletion in vivo is C independent. (A) In vitro C-dependent cytotoxicity of MB20 mAbs for spleen B cells. Values represent the mean (± SEM) percentage of $B220^+$ cells that were PI^+ in three or more experiments. (B) B cell depletion after MB20-11 (●) or isotype control (○) mAb treatment of $C3^{-/-}$, $C4^{-/-}$, or $C1q^{-/-}$ mice on day 0. Blood values indicate mean circulating B cell numbers (± SEM, per ml) before (time 0) and 1 h or 2, 4, or 7 d after mAb treatment (five or more mice per time point). Representative spleen B cell frequencies and mean B cell numbers (± SEM) 7 d after MB20-11 (solid bars) and isotype control (open bars) mAb treatment (five or more mice per group). (C and D) Blood and spleen B cell depletion after MB20-1 or MB20-18 (●) or isotype control (○) mAb treatment of $C3^{-/-}$ mice on day 0 compared with MB20-1 or MB20-18 (■) or isotype control (□) mAb treatment of WT mice on day 0. Representative spleen B cell depletion 7 d after MB20-1 or control mAb treatment of $C3^{-/-}$ littermates. Numbers indicate the percentage of $B220^+$ lymphocytes within the indicated gates. Bar graphs represent mean spleen B cell numbers (± SEM) 7 d after MB20-1 or isotype control mAb treatment of $C3^{-/-}$ (solid bars) or WT (open bars) mice (five or more mice per group). (A–D) Significant differences between mean results for MB20 or isotype control mAb–treated mice are indicated. *, $P < 0.05$; **, $P < 0.01$.

tivation contributed significantly to B cell depletion in vivo in this mouse model system (Fig. 4, B–D). Consistent with the current findings using genetically modified mice, previous in vivo studies found that C depletion had no effect on mAb-induced suppression of human melanoma and carcinoma in nude mice, whereas macrophage inactivation by silica treatment abolished tumor suppression (44). Studies using anti-CD8 mAbs have also documented the importance of FcγR in the clearance of $CD8^+$ cells and have shown that C activation is not necessary for the killing of $CD8^+$ cells in vivo (45, 46). Also consistent with anti-CD20 therapy primarily involving Ab-dependent cellular cytotoxicity, higher response rates are observed in lymphoma clinical trials when Rituximab therapy is combined with agents that enhance cellular cytotoxicity (47). Thus, tissue macrophages appear critical for B cell depletion after anti-CD20 mAb treatment.

Optimal anti-CD20 mAb-induced B cell depletion correlated closely with mAb isotype, with IgG2a > IgG1 > IgG2b >> IgG3 (Fig. 2 B and Table I). These isotype-specific effects of anti-CD20 mAbs correlate closely with FcγRI and FcγRIII specificities (38). In addition, anti-CD20 mAb therapy had modest, if any, effects in $FcR\gamma^{-/-}$ mice, but was effective in both $Fc\gamma RI^{-/-}$ and $Fc\gamma RIII^{-/-}$ mice (Fig. 3). The importance of mAb isotype in immunotherapy has long been appreciated, particularly for mouse IgG2a Abs (44, 46, 48–50). This suggests that monocyte expression of either high affinity FcγRI or low affinity FcγRIII is sufficient for B cell depletion. FcγRI function may actually dominate over FcγRIII function when IgG2a anti–mouse CD20 mAbs were used because blood and spleen B cell depletion were delayed or incomplete after MB20-11 mAb treatment in $Fc\gamma RI^{-/-}$ mice, but not in $Fc\gamma RIII^{-/-}$ mice (Fig. 3 A). The in vivo dependence of IgG2a mAb potency on FcγRI function has also been observed in other experimental systems (39, 51, 52). However, this result was unexpected because FcγRI normally appears to play a minor role in vivo because administered mAbs must compete with intrinsic circulating antibodies for high affinity FcγRI interactions (39, 52). Moreover, $Fc\gamma RIII^{-/-}$ and $FcR\gamma^{-/-}$ mice normally exhibit remarkably similar phenotypes during IgG-dependent immune responses (37). Thus, limited MB20-11 mAb binding to FcγRI may mediate efficient B cell phagocytosis due to high mAb potency, a high affinity for CD20, or its use at relatively high concentrations. Otherwise, MB20-11 mAb may effectively use the low affinity FcgRIII to mediate B cell depletion in the absence of FcγRI function as occurs with an IgG2a mAb reactive with RBCs in a mouse model of hemolytic anemia (53). Although FcγRI is reported to bind mouse IgG3 (54), IgG3 anti–mouse CD20 mAbs had little effect in vivo (Fig. 2 B). Extensive experiments to address the differential use of FcγRI or FcγRIII by anti-CD20 mAbs of different isotypes given at different doses are underway. In mice, FcγRII engagement inhibits effector cell activation, with genetic deletion of inhibitory FcγRs triggering increased susceptibility to immune complex–induced inflammation (55). Likewise, studies in CSF-1–deficient *op/op* mice have shown that i.v. γ globulin–mediated protection from pathogenic Ab-induced inflammation or thrombocytopenia is mediated through macrophage FcγRII (31, 56). Genetic deletion of inhibitory FcγRs also enhances in

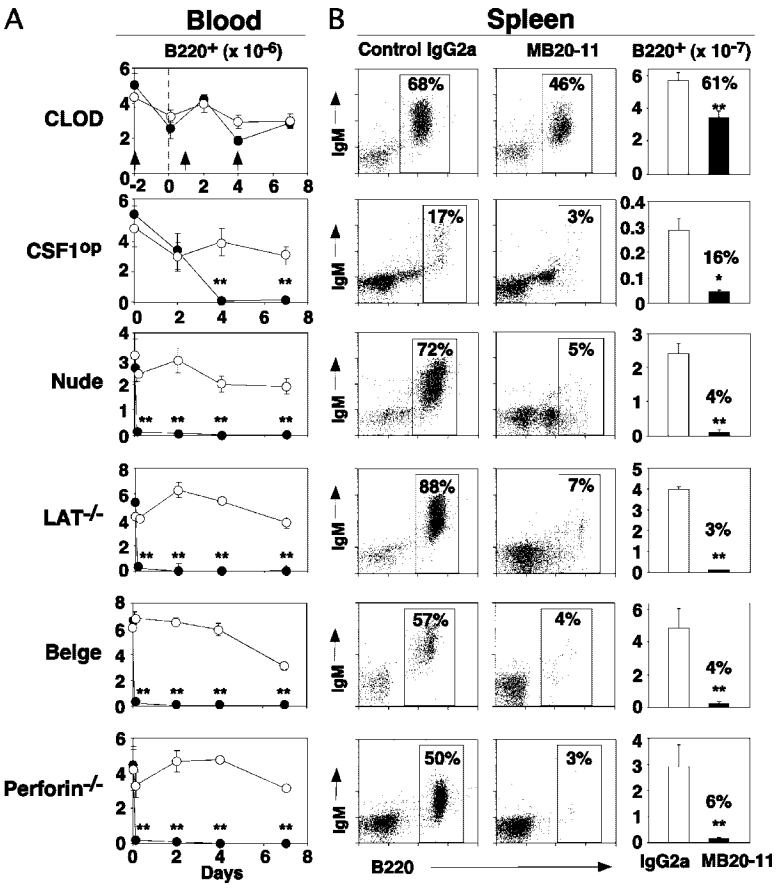

Figure 5. Monocytes mediate B cell depletion. WT mice were treated with clodronate (CLOD) as shown (arrows) to deplete macrophages, whereas other mice had genetic deficiencies in leukocyte subpopulations. (A) Blood B cell depletion after MB20-11 (●) or isotype control (○) mAb treatment on day 0. For clodronate-treated mice, blood B cell numbers were determined 1 h and 2, 4, and 7 d after mAb treatment, with the vertical dashed line indicating time 0 mAb treatment. For CSF1^{op} mice, circulating B cell numbers were not quantified 1 h after mAb treatment because of the small size of these mice and the risk for mortality. B cell numbers at 1-h time points are shown for the other mouse genotypes. (B) Representative flow cytometry analysis and mean spleen B cell numbers (± SEM) 7 d after MB20-11 (solid bars) or isotype control (open bars) mAb treatment (five or more mice per group). Significant differences between mean results from isotype control or MB20 mAb–treated cells are indicated. *, $P < 0.05$; **, $P < 0.01$.

vivo cytotoxicity against mAb-targeted tumors, including Rituximab targeting of human lymphoma cells in nude mice (26). Experiments to determine the extent that FcgRII expression influences B cell depletion by mouse anti–mouse CD20 mAbs of different isotypes given at different doses are underway because the current mechanistic immunotherapy studies using native mouse mAbs may differ from previous studies using chimerized or humanized mAbs bearing human Fc regions. Regardless, these results clearly demonstrate that strategies to augment monocyte FcγR expression and function in vivo should result in more effective immunotherapies (26). Moreover, the current observations corroborate studies in lupus and lymphoma patients showing that human FcγRIIa and FcγRIIIa polymorphisms correlate with the efficiency of tumor and B cell depletion during anti-CD20 mAb therapy (57–59). Consistent with an essential role for macrophages in B cell depletion after anti-CD20 mAb treatment, responses to Rituximab therapy also correlate with polymorphisms in human FcγRIIa, which is only expressed on macrophages and DCs (59). Collectively, these results indicate that the most important factor influencing anti-CD20 mAb efficacy in vivo is the mAb isotype and its capacity to interact with monocyte FcγR.

Although almost all of the anti–mouse CD20 mAbs in this study induced C-dependent killing in vitro (Fig. 4 A), there was no direct correlation between C activation in vitro and B cell depletion in vivo (Figs. 2 B and 4 A). Likewise, isotype-specific B cell depletion by the anti-CD20 mAbs contrasted with the relative abilities of the different anti-CD20 mAbs to initiate C-dependent cytotoxicity in vitro (Fig. 4 A) and the known isotype-specific abilities of mouse Abs to effectively activate mouse C, IgG2a > IgG2b > IgG3, but not IgG1 (60, 61). In vivo B cell depletion with anti-CD20 mAbs (Fig. 2 B) also contrasted with the isotype-specific abilities of mouse Abs to initiate C-dependent cytotoxicity (IgG2a = IgG2b > IgG3 > IgG1) of lymphoma cells in vivo (49). Although IgG2b and IgG3 mAbs are highly pathogenic, their effectiveness is due in part to their ability to induce C activation in addition to the ability of IgG2b mAbs to bind FcγRI and FcγRIII (51). IgG1 mAbs had low pathogenicity in this mouse model of Ab-induced anemia, but they were not effective in C activation. By contrast, IgG2b and IgG1 anti–mouse CD20 mAbs depleted blood and tissue B cells to the same extent in WT and $C3^{-/-}$ mice (Fig. 4, C and D), whereas IgG3 anti-CD20 mAbs had little effect on B cell numbers (Fig. 2 B). Thus, C activation does not appear to influence the efficacy of anti-CD20 mAbs in vivo. Similarly, FcγR-mediated erythrophagocytosis is the major pathogenic mechanism responsible for autoimmune hemolytic anemia in mice, with C-mediated hemolysis and erythrophagocytosis playing a minor, if any, role (39, 62, 63). Recently, the protective activities of Rituximab (human IgG1 chi-

mera) and the 1F5 (mouse IgG2a) anti–human CD20 mAbs in a mouse tumor model have been reported to be completely absent in $C1q^{-/-}$ mice (16). However, tissue B cell depletion by the MB20-11 IgG2a anti–mouse CD20 mAb was not affected by C1q deficiency (Fig. 4 B). Although simple explanations for these different results are not obvious, the fine specificities of different anti–human CD20 mAbs was recently reported to influence their in vivo effects (64). Although C activation by Rituximab and the 1F5 mAb is critical for lymphoma therapy in xenotransplantation models, the B1 (IgG2a) mAb was also effective but did not depend on C activation in vivo (64), although it effectively activates C in vitro (65). Furthermore, $F(ab')_2$ fragments of the B1 mAb, but not the 1F5 mAb, were therapeutically effective, indicating that non-Fc–dependent mechanisms are involved with the B1 mAb, which was able to induce higher levels of apoptosis than Rituximab and 1F5. Why these IgG2a anti–human CD20 mAbs have similar in vivo effects but are thought to use entirely different effector mechanisms is unclear. Moreover, both proposed mechanisms contrast with the mechanism of action of the IgG2a anti–mouse CD20 mAbs examined in this study. Perhaps these studies collectively demonstrate that in vitro measurements may not completely reflect what is relevant in vivo and that mAb activity in vitro may not predict in vivo function (45).

Although FcγR-mediated cytotoxicity appears to be the major effector mechanism for B cell depletion, factors in addition to mAb isotype and C activation are nonetheless important for mAb therapeutic efficacy. Additional important factors include the following: mAb affinity and avidity, mAb half-life in vivo, mAb effects on B cell function, the density and distribution of mAb binding sites on the target molecule, mAb effects on target molecule function (agonistic, antagonistic), and the efficiency of target molecule cross-linking by the mAb. Others have shown that CD20 density determines the in vitro susceptibility of malignant B cells to Rituximab and C (14). Because the density of individual mAbs binding to B cells (Table I and Fig. 1 C) did not correlate with their effectiveness for B cell depletion (Table I), this implies that mAb density on the cell surface is not the primary factor inducing optimal Ab-dependent cellular cytotoxicity–mediated clearance. Rather, the current studies demonstrate that mAb isotype is a more critical factor. Likewise, isotype-specific differences in mAb half-life did not correlate with anti-CD20 mAb-induced B cell depletion because mAb effectiveness was readily apparent within 48 h of treatment (Fig. 2 C) and IgG2b is cleared faster than IgG1 = IgG3 > IgG2a from serum (49). However, a longer mAb half-life in vivo is predicted to provide more durable B cell depletion in this model system. The efficiency of target molecule cross-linking by therapeutic mAbs and FcγR-expressing effector cells may also contribute to therapeutic outcome (66) because anti-CD20 mAb-induced signaling is often enhanced by hyper cross-linking (13, 67, 68). Thus, individual characteristics and the therapeutic advantages of each individual mAb would become more obvious if all 12 of the mAbs tested in this study had been of the same isotype. Nevertheless, heterogeneity between individual mAbs was demonstrated in this study with IgG2b anti-CD20 mAbs. For example, the MB20-18 mAb was effective at depleting both circulating and spleen B cells, whereas the MB20-7 mAb cleared most, but not all, circulating B cells and had only modest effects on spleen B cells. By contrast, the MB20-8 and MB20-10 mAbs did not induce rapid clearance of circulating B cells and did not affect spleen B cell numbers. The superior B cell depletion activity of the MB20-18 mAb relative to the other three IgG2b mAbs (Fig. 2 B) may relate to the fact that it bound to the surface of B cells at the highest levels of all anti–mouse CD20 mAbs (Table I and Fig. 1 C). Although the IgG2a and IgG1 anti-CD20 mAbs generally generated homogenous levels of B cell clearance, this is likely to reflect the fact that maximal B cell depletion was observed under the conditions tested. Thus, multiple factors affect the in vivo effectiveness of anti-CD20 mAb-induced B cell clearance, although mAb isotype was the most critical factor.

Human studies of anti-CD20 therapy are primarily focused on blood B cells or lymphoblastoid cell lines, rather than tissue B cells. However, the immunotherapy model used in this study indicates that although blood B cell depletion is rapid, it may not be an accurate indicator for anti-CD20 mAb effects on tissue B cells. For example, most anti-CD20 mAbs induced rapid depletion of circulating B cells within 1–48 h, whereas IgG2b and IgG3 anti-CD20 mAbs had modest, if any, effects on spleen B cells (Figs. 2, B and D, 3, and 4). Most circulating B cells did not reappear during these time periods, which strongly suggesting that they may have been killed and not merely sequestered. Because i.v. administration of clodronate liposomes preferentially depletes splenic and liver macrophages (35), and circulating B cells were not rapidly cleared in clodronate-treated mice (Fig. 5 A), the spleen and liver might be among the most likely sites for circulating and tissue B cell depletion. Rapid B cell depletion from blood is also observed in patients after anti-CD20 mAb infusion (10–12, 69). These results suggest that different B cell subpopulations may have different sensitivities to anti-CD20 therapy or that B cells present in different anatomical locations might be differentially affected. Alternatively, B cell depletion from the circulation may involve pathways in addition to FcγR-mediated phagocytosis or may reflect B cell migration into tissues rather than reflect B cell destruction. This possibility is supported by observations that some anti–human CD20 mAbs have potent physiologic effects on blood B cells and influence in vitro homotypic adhesion, Ca^{2+} influx, cell cycle regulation, and survival/apoptosis (1). Consistent with this, FcγRIIIa polymorphisms are not predictive of patient responses in chronic lymphocytic leukemia, which most commonly involves blood and marrow (70), whereas they are predictive of tumor clearance in follicular lymphomas (57, 59) where Ab-dependent cellular cytotoxicity appears critical (Figs. 3 and 4). Regardless, the current animal model allows these issues to be assessed di-

rectly and may provide additional understanding of the molecular mechanisms and pathways invoked during anti-CD20 therapy in vivo.

The use of 12 different anti-CD20 mAbs in this study has provided a unique opportunity to define the ability of individual mouse IgG isotopes in relation to B cell clearance and FcγR-dependent effector functions in the clearance of B cells during immunotherapy. Macrophage-mediated B cell depletion during anti-CD20 therapy has far-reaching clinical implications, which may also be applicable to other cell-directed mAb therapies. For example, augmenting monocyte numbers or function may increase anti-CD20 mAb effectiveness in vivo. In support of this concept, clinical studies showing that GM-CSF treatment or priming of neutrophils may improve the effectiveness of mAb-based therapies (71–74), although neutrophils were not implicated in anti-CD20 mAb depletion of B cells in this study. Similarly, immunotherapy effectiveness might be reduced in diseases with concomitant myelosuppression or immunosuppression, similar to the effects of clodronate on B cell depletion in this study (Fig. 5). Although early B cell depletion is observed in most patients with refractory non-Hodgkin's lymphoma after anti-CD20 therapy, only 40–60% of patients show a durable clinical response (75, 76). The unexplained high rate of failure for anti-CD20 therapy may in some cases result from concomitant myelosuppression or reduced numbers of tissue monocytes. This may also explain, in part, why disease progression can continue during mAb therapy despite continued CD20 expression by malignant cells (12). Variable depletion of effector monocytes may also explain why anti-CD20 mAb therapy is more effective as an initial therapy, in contrast to results obtained after patients relapse after chemotherapy (9). Because monocytes were found to provide a fundamental and essential mechanism for B cell depletion, there is critical need for a better understanding of monocyte function in patients with lymphoma and autoimmune disease undergoing mAb-based therapies.

We thank Drs. D. Steeber, Y. Liang, Y. Lee, W. St. Clair, M. Walport, and G. Kelsoe for their assistance.

These studies were supported by grants from the National Institutes of Health (CA96547 and AI56363), The Arthritis Foundation, and The Alliance for Lupus Research.

Submitted: 20 January 2004
Accepted: 29 April 2004

References

1. Tedder, T.F., and P. Engel. 1994. CD20: a regulator of cell-cycle progression of B lymphocytes. *Immunol. Today.* 15: 450–454.
2. Press, O.W., J.P. Leonard, B. Coiffier, R. Levy, and J. Timmerman. 2001. Immunotherapy of non-Hodgkin's lymphomas. *Hematology. (Am. Soc. Hematol. Educ. Program).* 2001:221–240.
3. Kaminski, M.S., K.R. Zasadny, I.R. Francis, A.W. Milik, C.W. Ross, S.D. Moon, S.M. Crawford, J.M. Burgess, N.A. Petry, G.M. Butchko, et al. 1993. Radioimmunotherapy of B-cell lymphoma with [^{131}I]anti-B1 (anti-CD20) antibody. *N. Engl. J. Med.* 329:459–465.
4. Weiner, L.M. 1999. Monoclonal antibody therapy of cancer. *Semin. Oncol.* 26:43–51.
5. Onrust, S.V., H.M. Lamb, and J.A. Balfour. 1999. Rituximab. *Drugs.* 58:79–88.
6. McLaughlin, P., C.A. White, A.J. Grillo-Lopez, and D.G. Maloney. 1998. Clinical status and optimal use of rituximab for B-cell lymphomas. *Oncology.* 12:1763–1769.
7. Silverman, G.J., and S. Weisman. 2002. Rituximab therapy and autoimmune disorders: prospects for anti-B cell therapy. *Arthritis Rheum.* 48:1484–1492.
8. Edwards, J.C.W., and G. Cambridge. 2001. Sustained improvement in rheumatoid arthritis following a protocol designed to deplete B lymphocytes. *Rheumatol.* 40:1–7.
9. Smith, M.R. 2003. Rituximab (monoclonal anti-CD20 antibody): mechanisms of action and resistance. *Oncogene.* 22: 7359–7368.
10. Reff, M.E., K. Carner, K.S. Chambers, P.C. Chinn, J.E. Leonard, R. Raab, R.A. Newman, and N. Hanna. 1994. Depletion of B cells in vivo by a chimeric mouse human monoclonal antibody to CD20. *Blood.* 83:435–445.
11. Maloney, D.G., A.J. Grillo-López, C.A. White, D. Bodkin, R.J. Schilder, J.A. Neidhart, N. Janakiraman, K.A. Foon, T.M. Liles, B.K. Dallaire, et al. 1997. IDEC-C2B8 (Rituximab) anti-CD20 monoclonal antibody therapy in patients with relapsed low-grade non-Hodgkin's lymphoma. *Blood.* 90:2188–2195.
12. Maloney, D.G., L.A. Grillo, D.J. Bodkin, C.A. White, T.M. Liles, I. Royston, C. Varns, J. Rosenberg, and R. Levy. 1997. IDEC-C2B8: results of a phase I multiple-dose trial in patients with relapsed non-Hodgkin's lymphoma. *J. Clin. Oncol.* 15:3266–3274.
13. Shan, D., J.A. Ledbetter, and O.W. Press. 1998. Apoptosis of malignant human B cells by ligation of CD20 with monoclonal antibodies. *Blood.* 91:1644–1652.
14. Golay, J., M. Lazzari, V. Facchinetti, S. Bernasconi, G. Borleri, T. Barbui, A. Rambaldi, and M. Introna. 2001. CD20 levels determine the in vitro susceptibility to rituximab and complement of B-cell chronic lymphocytec leukemia: further regulation by CD55 and CD59. *Blood.* 98:3383–3389.
15. Cragg, M.S., M.S. M., H.T. Chan, B.P. Morgan, A.V. Falatov, P.W. Johnson, R.R. French, and M.J. Glennie. 2003. Complement-mediated lysis by anti-CD20 mAb correlates with segregation into lipid rafts. *Blood.* 101:1045–1052.
16. Di Gaetano, N., E. Cittera, R. Nota, A. Vecchi, V. Grieco, E. Scanziani, M. Botto, M. Introna, and J. Golay. 2003. Complement activation determines the therapeutic activity of Rituximab in vivo. *J. Immunol.* 171:1581–1587.
17. Bellosillo, B., N. Villamor, A. López-Guillermo, S. Marcé, J. Esteve, E. Campo, D. Colomer, and E. Montserrat. 2001. Complement-mediated cell death induced by rituximab in B-cell lymphoproliferative disorders is mediated in vitro by caspase-independent mechanism involving the generation of reactive oxygen species. *Blood.* 98:2771–2777.
18. van der Kolk, L.E., A.J. Grillo-López, J.W. Baars, C.E. Hack, and M.H.J. van Oers. 2001. Complement activation plays a key role in the side-effects of rituximab treatment. *Br. J. Haematol.* 115:807–811.
19. Kennedy, A.D., M.D. Solga, T.A. Schuman, A.W. Chi, M.A. Lindorfer, W.M. Sutherland, P.L. Foley, and R.P. Taylor. 2003. An anti-C3b(i) mAb enhances complement activation, C3b(i) deposition, and killing of CD20$^+$ cells by ri-

tuximab. *Blood*. 101:1071–1079.
20. Treon, S.P., C. Mitsiades, N. Mitsiades, G. Young, D. Doss, R. Schlossman, and K.C. Anderson. 2001. Tumor cell expression of CD59 is associated with resistance to CD20 serotherapy in patients with B-cell malignancies. *J. Immunother.* 24:263–271.
21. Golay, J., L. Zaffaroni, T. Vaccari, M. Lazzari, G.M. Borleri, S. Bernasconi, F. Tedesco, A. Rambaldi, and M. Introna. 2000. Biologic response of B lymphoma cells to anti-CD20 monoclonal antibody rituximab in vitro: CD55 and CD59 regulate complement-mediated cell lysis. *Blood*. 95:3900–3908.
22. Di Gaetano, N., Y. Xiao, E. Erba, R. Bassan, A. Rambaldi, J. Golay, and M. Introna. 2001. Synergism between fludarabine and rituximab revealed in a follicular lymphoma cell line resistant to the cytotoxic activitiy of either drug alone. *Br. J. Haematol*. 114:800–809.
23. Weiner, G.J. 2003. Rituximab: complementary mechanisms of action. *Blood*. 101:788.
24. Weng, W.-K., and R. Levy. 2001. Expression of complement inhibitors CD46, CD55, and CD59 on tumor cells does not predict clinical outcome after rituximab treatment in follicular non-Hodgkin lymphoma. *Blood*. 98:1352–1357.
25. Anderson, D.R., A. Grillo-López, C. Varns, K.S. Chambers, and N. Hanna. 1997. Targeted anti-cancer therapy using rituximab, a chimeric anti-CD20 antibody (IDEC-C2B8) in the treatment of non-Hodgkin's B-cell lymphoma. *Biochem. Soc. Trans*. 25:705–708.
26. Clynes, R.A., T.L. Towers, L.G. Presta, and J.V. Ravetch. 2000. Inhibitory Fc receptors modulate in vivo cytoxicity against tumor targets. *Nat. Med*. 6:443–446.
27. Demidem, A., T. Lam, S. Alas, K. Hariharan, H. Hanna, and B. Bonavida. 1997. Chimeric anti-CD20 (IDEC-C2B8) monoclonal antibody sensitizes a B cell lymphoma cell line to cell killing by cytotoxic drugs. *Cancer Biother. Radiopharm*. 12:177–186.
28. Uchida, J., Y. Lee, M. Hasegawa, Y. Liang, A. Bradney, J.A. Oliver, K. Bowen, D.A. Steeber, K.M. Haas, J.C. Poe, et al. 2004. Mouse CD20 expression and function. *Int. Immunol*. 16:119–129.
29. Sato, S., N. Ono, D.A. Steeber, D.S. Pisetsky, and T.F. Tedder. 1996. CD19 regulates B lymphocyte signaling thresholds critical for the development of B-1 lineage cells and autoimmunity. *J. Immunol*. 157:4371–4378.
30. Zhou, L.-J., H.M. Smith, T.J. Waldschmidt, R. Schwarting, J. Daley, and T.F. Tedder. 1994. Tissue-specific expression of the human CD19 gene in transgenic mice inhibits antigen-independent B lymphocyte development. *Mol. Cell. Biol*. 14: 3884–3894.
31. Bruhns, P., A. Samuelsson, J.W. Pollard, and J. Ravetch. 2003. Colony-stimulating factor-1-dependent macrophages are responsible for IVIG protection in antibody-induced autoimmune disease. *Immunity*. 18:573–581.
32. Botto, M., M.C. Dell'Agnola, A.E. Bygrave, E.M. Thompson, H.T. Cook, F. Petry, M. Loos, P.P. Pandolfi, and M.J. Walport. 1998. Homozygous C1q deficiency causes glomerulonephritis associated with multiple apoptotic bodies. *Nat. Genet*. 19:56–59.
33. Zhang, W., C.L. Sommers, D.N. Burshtyn, C.C. Stebbins, J.B. DeJamette, R.P. Trible, A. Grinberg, H.C. Tsay, H.M. Jacobs, C.M. Kessler, et al. 1999. Essential role of LAT in T cell development. *Immunity*. 10:323–332.
34. Wessels, M.R., P. Butko, M. Ma, H.B. Warren, A. Lage, and M.C. Carroll. 1995. Studies of group B streptococcal infection in mice deficient in complement C3 or C4 demonstrate an essential role for complement in both innate and acquired immunity. *Proc. Natl. Acad. Sci. USA*. 92:11490–11494.
35. Van Rooijen, N., and A. Sanders. 1994. Liposome mediated depletion of macrophages: mechanism of action, preparation of liposomes and applications. *J. Immunol. Methods*. 174:83–93.
36. Gazzano-Santoro, H., P. Ralph, T.C. Ryskamp, A.B. Chen, and V.R. Mukku. 1997. A non-radioactive complement-dependent cytotoxicity assay for anti-CD20 monoclonal antibody. *J. Immunol. Methods*. 202:163–171.
37. Takai, T., M. Li, D. Sylvestre, R. Clynes, and J.V. Ravetch. 1994. FcR γ chain depletion results in pleiotrophic effector cell defects. *Cell*. 76:519–529.
38. Ravetch, J.V., and R.A. Clynes. 1998. Divergent roles for Fc receptors and complement in vivo. *Annu. Rev. Immunol*. 16: 421–432.
39. Fossati-Jimack, L., A. Ioan-Facsinay, L. Reininger, Y. Chicheportiche, N. Watanabe, T. Saito, F.M.A. Hofhuis, J.E. Gessner, C. Schiller, R.E. Schmidt, et al. 2000. Markedly different pathogenicity of four immunoglobulin G isotype-switch variants of an antierythrocyte autoantibody is based on their capacity to interact in vivo with the low-affinity Fcγ receptor III. *J. Exp. Med*. 191:1293–1302.
40. Hazenbos, W.L.W., J.E. Gessner, F.M.A. Hofhuis, H. Kuipers, D. Meyer, I.A.F.M. Heijnen, R.E. Schmidt, M. Sandor, P.J.A. Capel, M. Daëron, et al. 1996. Impaired IgG-dependent anaphylaxis and Arthus reaction in FcγRIII (CD16) deficient mice. *Immunity*. 5:181–188.
41. Cecchini, M.G., M.G. Dominguez, S. Mocci, A. Wetterwald, R. Felix, H. Fleisch, O. Chisholm, W. Hofstetter, J.W. Pollard, and E.R. Stanley. 1994. Role of colony stimulating factor-1 in the establishment and regulation of tissue macrophages during postnatal development of the mouse. *Development*. 120:1357–1372.
42. Kagi, D., B. Ledermann, K. Burki, P. Selleer, B. Odermatt, K.J. Olsen, E.R. Podack, R.M. Zinkernagel, and H. Hengartner. 1994. Cytotoxicity mediated by T cells and natural killer cells is greatly impaired in perforin-deficient mice. *Nature*. 369:31–37.
43. Dyall, R., L.V. Vasovic, R.A. Clynes, and J. Nikolic-Zugic. 1999. Cellular requirements for the monoclonal antibody-mediated eradication of an established solid tumor. *Eur. J. Immunol*. 29:30–37.
44. Herlyn, D., and H. Koprowski. 1982. IgG2a monoclonal antibodies inhibit human tumor growth through interaction with effector cells. *Proc. Natl. Acad. Sci. USA*. 79:4761–4765.
45. Isaacs, J.D., M.R. Clark, J. Greenwood, and H. Waldmann. 1992. Therapy with monoclonal antibodies. An in vivo model for the assessment of therapeutic potential. *J. Immunol*. 148:3062–3071.
46. Isaacs, J.D., J. Greenwood, and H. Waldmann. 1998. Therapy with monoclonal antibodies. II. The contribution of Fcγ receptor binding and the influence of C_H1 and C_H3 domains on in vivo effector function. *J. Immunol*. 161:3862–3869.
47. Ansell, S.M., T.E. Witzig, P.J. Kurtin, J.A. Sloan, D.F. Jelinek, K.G. Howell, S.N. Markovic, T.M. Habermann, G.G. Klee, P.J. Atherton, et al. 2002. Phase 1 study of interleukin-12 in combination with rituximab in patients with B-cell non-Hodgkin lymphoma. *Blood*. 99:67–74.
48. Kaminski, M.S., K. Kitamura, D.G. Maloney, M.J. Campbell, and R. Levy. 1986. Importance of antibody isotype in monoclonal anti-idiotype therapy of a murine B cell lymphoma. A study of hybridoma class switch variants. *J. Immunol*. 136:1123–1130.
49. Denkers, E.Y., C.C. Badger, J.A. Ledbetter, and I.D. Bern-

stein. 1985. Influence of antibody isotype on passive serotherapy of lymphoma. *J. Immunol.* 135:2183–2186.
50. Liu, A.Y., R.R. Robinson, E.D. Murray, Jr., J.A. Ledbetter, I. Hellströom, and K.E. Hellström. 1987. Production of a mouse-human chimeric monoclonal antibody to CD20 with potent Fc-dependent biologic activity. *J. Immunol.* 139:3521–3526.
51. Azeredo da Silveira, S., S. Kikuchi, L. Fossati-Jimack, T. Moll, T. Saito, J.S. Verbeek, M. Botto, M.J. Walport, M. Carroll, and S. Izui. 2002. Complement activation selectively potentiates the pathogenecity of the IgG2b and IgG3 isotypes of a high affinity anti-erythrocyte autoantibody. *J. Exp. Med.* 195:665–672.
52. Ioan-Facsinay, A., S.J. de Kimpe, S.M.M. Hellwig, P.L. van Lent, F.M.A. Hofhuis, H.H. van Ojik, C. Sedlik, S.A. da Silveira, J. Gerber, Y.F. de Jong, et al. 2002. FcγRI (CD64) contributes substantially to severity of arthritis, hypersensitivity responses, and protection from bacterial infection. *Immunity.* 16:391–402.
53. Fossati-Jimack, L., L. Reininger, Y. Chicheportiche, R. Clynes, J.V. Ravetch, T. Honjo, and S. Izui. 1999. High pathogenic potential of low-affinity autoantibodies in experimental autoimmune hemolytic anemia. *J. Exp. Med.* 190:1689–1696.
54. Gavin, A.L., N. Barnes, H.M. Dijstelbloem, and P.M. Hogarth. 1998. Cutting edge: identification of the mouse IgG3 receptor: implications for antibody effector function at the interface between innate and adaptive immunity. *J. Immunol.* 160:20–23.
55. Dijstelbloem, H.M., J.G.J. van de Winkel, and C.G.M. Kallenberg. 2001. Inflammation in autoimmunity: receptors for IgG revisited. *Trends Immunol.* 22:510–516.
56. Samuelsson, A., T.L. Towers, and J.V. Ravetch. 2001. Anti-inflammatory activity of IVIG mediated through the inhibitory Fc receptor. *Science.* 291:484–486.
57. Cartron, G., L. Dacheux, G. Salles, P. Solal-Celigny, P. Bardos, P. Colombat, and H. Watier. 2002. Therapeutic activity of humanized anti-CD20 monoclonal antibody and polymorphism in IgG Fc receptor FcγRIIIa gene. *Blood.* 99:754–758.
58. Anolik, J.H., D. Campbell, R.E. Felgar, F. Young, I. Sanz, J. Rosenblatt, and R.J. Looney. 2003. The relationship of FcgRIIIa genotype to degree of B cell depletion by rituximab in the treatment of systemic lupus erythematosus. *Arthritis Rheum.* 48:455–459.
59. Weng, W.-K., and R. Levy. 2003. Two immunoglobulin G fragment C receptor polymorphisms independently predict response to rituximan in patients with follicular lymphoma. *J. Clin. Oncol.* 21:3940–3947.
60. Neuberger, M.S., and K. Rajewsky. 1981. Activation of mouse complement by monoclonal mouse antibodies. *Eur. J. Immunol.* 11:1012–1016.
61. Klaus, G.G., M.B. Pepys, K. Kitajima, and B.A. Askonas. 1979. Activation of mouse complement by different classes of mouse antibody. *Immunology.* 38:687–695.
62. Meyer, D., C. Schiller, J. Westermann, S. Izui, W.L.W. Hazenbos, J.S. Verbeek, R.E. Schmidt, and J.E. Gessner. 1998. FcgRIII (CD16)-deficient mice show IgG isotype dependent protection to experimental autoimmune hemolytic anemia. *Blood.* 92:3997–4002.
63. Sylvestre, D.L., R. Clynes, M. Ma, H. Warren, M.C. Caroll, and J.V. Ravetch. 1996. Immunoglobulin G–mediated inflammatory responses develop normally in complement-deficient mice. *J. Exp. Med.* 184:2385–2392.
64. Cragg, M.S., and M.J. Glennie. 2004. Antibody specificity controls in vivo effector mechanisms of anti-CD20 reagents. *Blood.* 103:2738–2743.
65. Nadler, L.M., T. Takvorian, L. Botnick, R.C. Bast, R. Finberg, S. Hellman, G.P. Canellos, and S.F. Schlossman. 1984. Anti-B1 monoclonal antibody and complement treatment in autologous bone-marrow transplantation for relapsed B-cell non-Hodgkin's lymphoma. *Lancet.* 2:427–431.
66. Reddy, M.P., C.A.S. Kinney, M.A. Chaikin, A. Payne, J. Fishman-Lobell, P. Tsui, P.R. Dal Monte, M.L. Doyle, M.R. Brigham-Burke, D. Anderson, et al. 2000. Elimination of Fc receptor-dependent effector functions of a modified IgG4 monoclonal antibody to human CD4. *J. Immunol.* 164:1925–1933.
67. Mathas, S., A. Rickers, K. Bommert, B. Dorken, and M.Y. Mapara. 2000. Anti-CD20- and B-cell receptor-mediated apoptosis: evidence for shared intracellular signaling pathways. *Cancer Res.* 60:7170–7176.
68. Shan, D., J.A. Ledbetter, and O.W. Press. 2000. Signaling events involved in anti-CD20-induced apoptosis of malignant human B cells. *Cancer Immunol. Immunother.* 48:673–683.
69. Winkler, U., M. Jensen, O. Manzke, H. Schulz, V. Diehl, and A. Engert. 1999. Cytokine-release syndrome in patients with B cell chronic lymphocytic leukemia and high lymphocyte counts after treatment with an anti-CD20 monoclonal antibody (Rituximab, IDEC-C2B8). *Blood.* 94:2217–2224.
70. Farag, S.S., I.W. Flinn, R. Modali, T.A. Lehman, D. Young, and J.C. Byrd. 2004. FcγRIIIa and FcγRIIa polymorphisms do not predict response to rituximab in B-cell chronic lymphocytic leukemia. *Blood.* 103:1472–1474.
71. Stockmeyer, B., M. Schiller, R. Repp, H.M. Lorenz, J.R. Kalden, M. Gramatzki, and T. Valerius. 2002. Enhanced killing of B lymphoma cells by granulocyte colony-stimulating factor-primed effector cells and Hu1D10-a humanized human leukocyte antigen DR antibody. *Brit. J. Haematol.* 118:959–967.
72. van der Kolk, L.E., M. de Haas, A.J. Grillo-Lopez, J.W. Baars, and M.H. van Oers. 2002. Analysis of CD20-dependent cellular cytotoxicity by G-CSF-stimulated neutrophils. *Leukemia.* 16:693–699.
73. Stockmeyer, B., D. Elsasser, M. Dechant, R. Repp, M. Gramatzki, M.J. Glennie, J.G. van de Winkel, and T. Valerius. 2001. Mechanisms of G-CSF- or GM-CSF-stimulated tumor cell killing by Fc receptor-directed bispecific antibodies. *J. Immunol. Methods.* 248:103–111.
74. Elasser, D., T. Valerius, R. Repp, G.J. Weiner, Y. Deo, J.R. Kalden, J.G. van de Winkel, G.T. Stevenson, M.J. Glennie, and M. Gramatzki. 1996. HLA class II as potential target antigen on malignant B cells for therapy with bispecific antibodies in combination with granulocyte colony-stimulating factor. *Blood.* 87:3803–3812.
75. Coiffier, B., C. Haioun, N. Ketterer, A. Engert, H. Tilly, D. Ma, P. Johnson, A. Lister, M. Feuring-Buske, J.A. Radford, et al. 1998. Rituximab (anti-CD20 monoclonal antibody) for the treatment of patients with relapsing or refractory aggressive lymphoma: a multicenter phase II study. *Blood.* 92:1927–1932.
76. McLaughlin, P., L.A. Grillo, B.K. Link, R. Levy, M.S. Czuczman, M.E. Williams, M.R. Heyman, B.I. Bence, C.A. White, F. Cabanillas, et al. 1998. Rituximab chimeric anti-CD20 monoclonal antibody therapy for relapsed indolent lymphoma: half of patients respond to a four-dose treatment program. *J. Clin. Oncol.* 16:2825–2833.